Flexible electro-responsive in-situ polymer acid doped polyaniline membranes for permeation enhancement and membrane fouling removal

Li Li Xu,[1,2,3] Salman Shahid,[1,2], Darrell Alec Patterson[1,2], Emma Anna Carolina Emanuelsson[1*]

1. Department of Chemical Engineering, University of Bath, Bath, United Kingdom, BA2 7AY.
2. Centre for Advanced Separations Engineering, University of Bath, Bath, United Kingdom, BA2 7AY.
3. National Engineering Laboratory for Industrial Wastewater Treatment, Research Centre for Eco-Environmental Sciences, Chinese Academy of Sciences, 18 Shuangqing Road, Beijing, 100085, China

*Corresponding author: E.A.Emanuelsson-Patterson@bath.ac.uk

This study investigates the performance of a new electrically tuneable polyaniline (PANI) membrane, and shows that this synthesis method has the potential to address key challenges of small-acid doped PANI membranes, including: acid dopants leaching out during filtration and low mechanical strength. The novel in-situ polymerisation used poly (2-acrylamido-2-methyl-1-propanesulfonic acid) (PAMPSA), as polymer acid template leads to the formation of inter-polymer complexes of PANI and polymer acid. The developed membranes were comprehensibly evaluated through visual, chemical, mechanical and filtration studies and compared to small-acid doped membranes (PANI-HCl membranes). The PANI-PAMPSA membranes were smooth, acid leach resistant, had higher tensile strength and showed conductivity three magnitudes higher compared to PANI membrane with post cast doping. The developed membrane showed in-filtration performance stability, electrical tuneability (in-situ control of flux and rejection) and fouling removal characteristics under applied electrical potential. Data obtained by SEM, IR spectroscopy, electrical analysis and cross-flow filtration confirm these results. The overall results showed that the proposed membrane fabrication procedure resulted in a significant improvement in performance across a range of critical parameters, including conductivity, stability, flexibility, permeance and fouling removal with additional advantage of being electrically tuneable.

Keywords: polyaniline, polymer acid dopant, electrically tuneable membrane, stimuli responsive membrane, anti-fouling.

1 Introduction

Conventional membranes cannot have their transport properties tuned in-situ, as their properties are fixed during or after fabrication (i.e. polymer type, pore size, surface charge, microstructure) [1-3], resulting in issues such as weakened

separation performance over time, membrane fouling and limited ability to change the membrane properties with changing feeds. Thus there is a need for developing tuneable membranes (so called stimuli-responsive membranes) which can change the transport properties in-situ to create new opportunities for membrane applications. There are a range of external stimuli, such as pH, temperature, light, magnetic field, *etc*. [4-7]. More recently, applying an electrical potential has shown to be able to finely tune properties and achieve pulsatile drug release, ion transport and fouling removal [8-10].

Polyaniline (PANI), as an intrinsically conducting polymer, is particularly attractive, since its porosity can be controlled at a molecular level through simple acid/base doping/dedoping [11, 12]. It has also been shown that the transport property of small-acid doped PANI membranes can be changed in-situ by applying an external electrical potential across the membrane[13, 14]. However, two main problems exist with these conventional small-acid doped PANI membranes: the acids leaching out during filtration and low mechanical strength [14-18].

To overcome these challenges, various long chain and organic polymer acids (PAs) have been used as dopants, including poly(2-acrylamido-2-methyl-1-propanesulfonic acid) (PAMPSA) [19, 20], poly(acrylic acid) (PAAc) [16, 21, 22], poly(methyl vinyl ether-alt-maleic acid) (PMVEA) [23], poly(styrenesulfonic acid) (PSSA) [18, 24], *etc*. PAs enable the formation of a double-stranded structure with PANI, due to the strong intermolecular interactions between acid groups and imine nitrogen which can reduce acid leaching [25]. PA dopants also act as plasticisers which make the membranes less brittle [18, 25]. The improved flexibility allows these membranes to be more easily handled and used [18, 26]. PAs have also shown improved properties (wider range of solubility, processibility) as well as additional functionalities to the resulting materials [17, 25, 27].

PAs can be incorporated into the PANI structure by several different methods, including chemical oxidation, electrochemical polymerisation and enzymatic synthesis [19, 20, 28, 29]. Chemical oxidation of aniline with PAs serving is one of the most common methods due to its simplicity and low cost [30]. This approach involves the binding of the aniline monomer into PA templates, and then polymerising anilinium cations on the PA templates to obtain the PA doped PANI complex (PANI-PA), ensuring a strong incorporation and binding of any size of PA dopants into the PANI structure [20, 23, 31]. Such complexes have previously been investigated in the literature for potential applications in biosensor, ammonia optical sensor, but without investigating the electrical tuneability. PANI-PA membranes have so far been produced by adding the PA after the PANI has been synthesised. This includes: blending undoped PANI with acids before membrane fabrication, adding acids in the casting solution during membrane preparation and secondary doping with acids after membrane preparation [17, 21, 22, 32-35]. The first and third methods require the separate synthesis of PANI (typically with a small-acid), which then needs to be dedoped by ammonia and then redoped by the desired acids. These two methods have three disadvantages: it is time consuming, complicated and potentially ineffective, since the bulky acids cannot diffuse completely into the tight membrane structure, which therefore decreases the doping efficiency and membrane conductivity. The second method - adding acids in the casting solution during membrane preparation - generally produces a membrane with disordered polymer packing and random distribution of acids [36], which is not suitable for producing a membrane with consistent properties and therefore separation performance across the membrane sheet. To overcome these issues, we are proposing a novel fabrication method: PA is incorporated into PANI structure which starts with the chemical oxidation of aniline on the template of PAs. The obtained PANI-PA complex will then be directly used to prepare the membrane. There will be no need for a dedoping and redoping process. We

hypothesise that the acid dopants already incorporated in the membrane will create a stronger bond than if the PANI was synthesised and then secondary doped. Since the PANI-PA is synthesised together, this new method can also overcome the challenges of having to get penetration of bulky acids into a tight membrane structure during secondary doping and so, in theory, it should also increase the dopant loading compared to secondary doping with PAs. Compared with adding acids in the casting solution, the proposed method is expected to grow polyaniline along the PA template, producing a tightly bound double stranded PANI-PA structure and a more ordered packing of the PANI-PA structure which should ultimately produce a more uniformly doped PANI membrane [31].

Therefore, the aims of this paper are:

(i) To determine for the first time if a defect free membrane (PANI-PAMPSA membranes) can be formed from in-situ synthesised PAMPSA doped PANI (PANI-PAMPSA) complex.

(ii) To determine if PANI-PAMPSA membranes can overcome acid dopant leaching during fluid filtration and membrane brittleness. The PANI-PAMPSA membranes will be compared to small-acid (HCl) doped PANI membranes (PANI-HCl membrane).

(iii) To investigate the tuneability, and thus potential applications of the in-situ synthesised PANI-PAMPSA membranes, by comparing the electrically stimuli-response properties of the different PANI membranes.

Change in flux and rejection will be investigated using a bespoke in-house cross-flow rig with electrodes in contact with the surface of the membrane with a solution of mixed PEG oligomers as rejection probes.

Potential for anti-fouling will be investigated using bovine serum albumin (BSA) as the model foulant.

2 Experimental

2.1 Materials

Aniline, hydrochloric acid (HCl), acetonitrile (HPLC grade), ammonium persulfate (APS), N-methyl-2-pyrrolidone (NMP), 4-methyl piperidine (4-MP), BSA, poly(acrylic acid)/PAAc (MW=450,000 g mol^{-1}, powder), poly(styrenesulfonic acid)/PSSA (MW=75,000 g mol^{-1}, 18 wt% in water) and poly(methyl vinyl ether-alt-maleic acid)/PMVEA (MW=80,000 g mol^{-1}, powder) were obtained from Sigma-Aldrich (UK). Acetone, PAMPSA, fluorescein isothiocyanate (FITC) were purchased from Fisher (UK). All solutions were prepared with deionised (DI) water taken from a Purelab Option unit.

2.2 Synthesis of PANI-PAMPSA and PANI-HCl complex

Aniline (0.06 mol), at 4:1 monomer to acid (PAMPSA or HCl) repeat unit molar ratio, was dissolved in the 150 mL acid solution (0.1 M). 0.06 mol of ammonium persulfate (1.56 M) in deionised water (38.4 mL), was added into the mixture of aniline and acid by peristaltic pump with a speed of 20 mL h^{-1} to give a 1:1 APS to aniline monomer molar ratio. The polymerisation temperature was set at 15°C and the reaction time was 24 h. The reactant product was washed with 6× 250 mL of DI water and 3× 250 mL of acetone, and then dried in a vacuum oven at 60°C for 24 h. The obtained complex was ground by mortar and pestle to give a fine black green product. Fig S1 (Supplementary material) shows the setup used for the synthesis (chemical polymerisation) of PANI-PAMPSA and PANI-HCl complex

2.3 PANI membrane fabrication

2.3.1 In-situ polymerised PANI-PAMPSA membranes

The non-solvent induced phase separation (NIPS) method was used to prepare all membranes with DI water as the coagulation bath at room temperature. To prepare the membrane dope solution, PANI-PAMPSA (5.78 g, 20 wt%) was added in small portions to the mixture of NMP (20.64 mL) and 4-MP (2.35 mL) using a funnel (1 h). The mixture was stirred at 300 rpm for 4 h until a homogeneous solution was achieved and then at 100 rpm overnight. Thereafter, vacuum was used to remove air bubbles for 3 min. The membrane was cast as per Xu *et al.* [14]. Briefly, a polyethylene/polypropylene mixture backing layer (Novatexx 2431) was immobilised on a flat glass plate before casting. An adjustable casting knife (Elcometer 3700) was used to cast 250 μm membranes with Elcometer 4340 automatic film applicator. The membrane was formed after immersion precipitation in DI water bath at room temperature. Fig S2 (Supplementary material) shows the membrane preparation process. To determine the wider applicability of this method to PAs, another three different PAs were also trialled: poly(styrenesulfonic acid) (PSSA), poly(methyl vinyl ether-alt-maleic acid) (PMVEA) and poly(acrylic acid) (PAAc) were utilised to synthesise PANI-PA complex and the PANI-PA complex were then used to form membranes by NIPS. Table S1 (Supplementary material) outlines the membrane fabrication results by the four types of PANI-PA complex. PANI-PAMPSA alone, under the casting conditions and solvents considered, was able to form a membrane with a flat, defect free surface and good adhesion to the support layer.

2.3.2 HCl doped PANI membranes (PANI-HCl membranes)

The casting solution with the HCl doped PANI (PANI-HCl) complex gelled in the dissolution process and thus primary doped PANI-HCl membranes could not be

prepared in the same way as the PANI-PAMPSA membranes. Therefore, the PANI-HCl complex was firstly dedoped using ammonia to form PANI-EB (undoped PANI). Briefly, the PANI-HCl complex was stirred in 250 mL ammonia solution (33.3%, w/v) for about 12 h and then washed with 3× 500 mL deionised water to remove the excess ammonia. After that, the polymer was dried by vacuum filtration at room temperature for 24 h. The casting was then performed as in Section 2.3.1 to produce an undoped PANI membrane (PANI-EB membrane). The PANI-EB was then doped through immersion membrane pieces (approximately 3× 15 cm^2) in 0.1 M HCl solution (50 mL) for 24 h to form PANI-HCl doped membrane.

2.4 Membrane Characterisation

2.4.1 FTIR analysis

FTIR spectra of samples were recorded from 4000 to 650 cm^{-1} using a PerkinElmer Spectrum 100™ - FTIR Spectrometer fitted with an attenuated total reflectance (ATR) detector. The spectra were collected by using 32 scans at 4 cm^{-1} resolution. All samples were dried at 40°C before observation.

2.4.2 Morphology analysis

The samples were imaged by SEM (JSM-6301F, JEOL, Germany) or FESEM (JSM-6480 LV, JEOL, Germany). Energy dispersive spectroscopy (EDS) was used to determine the elemental compositions of the PANI-EB and PANI-PAMPSA complex (powder). Membrane samples were prepared by cutting the membrane into small pieces and fracturing a cross-section in liquid nitrogen. Samples were mounted on stubs using double sided tape and samples imaged by FSEM were sputter coated with chromium (Q150T S, Quorum) under argon flow and samples imaged by SEM were sputter coated with gold (Edwards 150B, UK) before imaging. The samples imaged by FSEM used an acceleration voltage of 2 and 5 kV and the samples imaged by SEM used an acceleration voltage of 10 kV.

2.4.3 Membrane surface conductivity analysis

The resistivity of samples was measured using a JANDEL RM300 conductivity meter at room temperature. The calculation was followed a published paper and conductivity is the inverse of resistivity [14]. The conductivity represents the average of a minimum of 10 times.

2.4.4 Membrane mechanical properties analysis

The mechanical properties of the membranes were evaluated using an Instron model 3369 tester. Membrane samples were cut into rectangular strips of approximately 5 × 75 mm using a razor blade. The samples were gripped by clamps and a pull speed of 2 mm min^{-1} used to perform the test. Thickness of the membrane was determined by standard Vernier callipers. At least three membrane samples were recorded and averaged.

2.4.5 Membrane transport property analysis

Dead-end filtration was performed in a Sterlitech HP 4750 stirred stainless steel cell (USA), which has an effective membrane area of 14.6 cm^2. A magnetic stirrer was used to minimise concentration polarisation with a stirring speed of 300 rpm. The cell was placed in a 25°C water bath. Pressure (2 bar) was supplied using nitrogen gas (BOC, UK). The membranes were conditioned by permeating DI water under pressure until constant flux was achieved. DI water or polyethylene glycols (PEGs) mixtures (of PEG 1000, 1500, 2000, 3000, 4000 and 6000) as per [37] were added into the filtration cell and the permeate was collected in a measuring cylinder. Permeate mass versus time was recorded by using a computer operated digital mass balance (Sartorius LC3201D-00M, Germany) to determine the permeate mass flux. High-performance liquid chromatography (HPLC) equipped with an evaporative light scattering detector (ELSD) was used to determination of the concentration of individual PEG oligomers in the feed,

permeate and retentate. Rejection of each PEG oligomer was determined using Equation 1:

$$R_{\mathrm{j}}(\%) = \left(1 - \frac{C_{\mathrm{p}}}{C_{\mathrm{f}}}\right) \times 100\% \qquad \text{Equation 1}$$

Where R_j is the membrane rejection, C_f is the PEG oligomer concentration in the feed and C_p is the PEG oligomer concentration in the permeate. Rejection of each PEG oligomer was plotted vs molecular weight. See [37] for the full detail of the procedure.

2.4.6 Electrical tuneability analysis

Fig S3 (Supplementary material) shows the electrically connected cross-flow filtration setup. The setup contains two PTFE cross-flow electro-filtration cells with an active area of 14.6 cm^2 based on commercial stainless steel cells [13, 14]. The operating pressure was provided using a precision metering pump (G10XKSGHFEMH, Michael Smith Engineering, UK). Two stainless steel electrodes were applied to supply electrical contact between electrodes and the membrane surface. The electrical potential was provided by a Weir 431D power supply. Current was measured by a Maplin UT58C digital multi-meter. The temperature was kept at 25°C by a water bath.

In a typical experiment, 1.5 L of DI water or PEG mixture (PEG 1000, 1500, 2000, 3000, 4000 and 6000) [37] was circulated at 1.2 L min^{-1} (a flowrate that was not too high to cause an unstable operating pressure but not too low to lead to membrane fouling). To test the electrical tuneability, the permeance and MWCO of the membranes were compared with and without an applied potential of 30 V. The first sample of permeate (t = 0 min) was taken after constant pressure was continued. Further samples of permeate were obtained at 30, 60 and 120 min intervals after the first sample. Sample analysis was as per Section 2.4.5.

231 Membrane flux was calculated from the permeate mass versus time data recorded
232 by using a computer operated digital mass balance (A&D Instruments, GR-300,
233 UK).

234 **2.5 Fouling test and post-fouling characterisation**

235 The potential for these membranes to defouling under an applied potential at
236 room temperature was examined using a static rig (Fig S4 in the Supplementary
237 material). To foul the PANI-PAMPSA membranes, dead-end filtration was used.
238 Membranes were firstly preconditioned with DI water, and then 200 mL of DI
239 water was used to determine the flux of virgin membranes, after that 200 mL of
240 1.0 g L^{-1} BSA solution was added to the cell to foul the membrane, and then 200
241 mL of DI water was run again to measure the flux of the fouled membranes.

242 To determine the efficacy of applied potential across these membranes for
243 removing the foulant, the BSA fouled membranes were firstly immersed in 800 mL
244 water in a beaker (the wash solution), and then an external potential of 30 V was
245 applied on the membrane for up to 120 min. The samples of the wash solution
246 were taken at 0, 30, 60, 90 and 120 min. Membranes following this treatment are
247 as termed "cleaned". UV-Vis (200 to 900 nm) was used to analyse the components
248 of the wash solution to evaluate membrane defouling behaviour by the application
249 of external potential. In addition, two control experiments were also run on BSA
250 fouled membranes in the absence of applied potential and an unfouled membrane
251 in the presence of applied potential. Dead-end filtration was then again used to
252 measure the permeance of the cleaned membranes with 200 mL of DI water.

253 SEM (JSM-6480LV, JEOL, Germany) as per Section 2.4.2 and CSLM (Carl Zeiss LSM,
254 Germany) was utilised to determine the surface difference among virgin, fouled
255 and cleaned PANI-PAMPSA membranes and distinguish the membrane defouling
256 action with applied potential. For CSLM characterisation, samples were stained

using FITC dye for 1 h and then washed with phosphate-buffered saline to remove the excess dye.

3 Results and Discussion

3.1 Membrane fabrication from in-situ synthesised PANI-PAMPSA

3.1.1 Preparation of PANI-PAMPSA membranes

A range of polymer acids (e.g. PAMPSA, PSSA, PMVEA and PAAc) were initially chosen to synthesise the PANI-PA complex (Table S1 in the Supplementary material). PAMPSA with the properties shown in **Error! Reference source not found.** was selected as among the four polymer acids it was the only polymer acid that led to the formation of a membrane with a flat, defect free surface with good adhesion to the support layer. Also, PAMPSA has a flexible backbone that can adapt to the rigid conjugated structure of PANI, which allows the formation of a strongly bound double-stranded interpolymer complex with PANI [19, 29].

Table 1 The properties of PAMPSA.

Polymer acid	Chemical structure	MW (g mol^{-1})	Physical form	pH (0.1 M)
PAMPSA	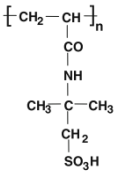	800, 000	10 wt% in water	2.0±0.1

PAMPSA possesses a highly flexible backbone of which its conformation can be adjusted to match the rigid conjugated macromolecule of PANI [19, 29]. The electrical conductivity of the PANI-PAMPSA complex (powder) was 1.2 ×10^{-1} S cm^{-1} which suggests that incorporation of PAMPSA into PANI structure has occurred and delocalised polarons can be formed in the PANI-PAMPSA complex (powder), allowing charge transfer along the polymer chains. This allows the PAMPSA chain

to form a strong interaction with PANI during the in-situ polymerisation. In comparison, when using the traditional methodology of secondary doping of PAMPSA, the conductivity was 3.0×10^{-4} S cm^{-1}, three orders of magnitude lower than that of the PANI-PAMPSA complex (powder) formed by in-situ polymerisation. This is due to the large molecular weight of the PAMPSA as there are significant diffusion resistances for it to diffuse fully into the PANI structure [17, 20]. Therefore, we confirm the hypothesis that in-situ synthesis of PANI with PAMPSA is more effective at incorporating PAMPSA into the PANI structure to obtain a PANI-PAMPSA complex (powder) with a high electrical conductivity.

The PANI-PAMPSA complex (powder) formed a viscous solution when mixed with the NMP casting solvent and produced a flat and shiny membrane surface when immersed in the water bath (Table S1 in the Supplementary material). In comparison, PANI-HCl gelled during dissolution which suggests that the incorporation of PAMPSA into the PANI structure improves solution processability. This is consistent with previous studies that suggest that the presence of PA macromolecules within conducting polymers allows the formation of different structures and morphologies for PANI, which can bring improved properties (such as a wider range of solubility, improved processibility) as well as additional functionalities to the resulting materials [17, 25, 27].

3.1.2 FTIR analysis of the PANI-PAMPSA complex (powder) and PANI-PAMPSA membrane

Fig. 1 shows the FTIR spectra for the PANI-PAMPSA complex (powder) and undoped PANI (PANI-EB) (with detailed peak information in Table S2 (Supplementary material)). It shows that the PANI-EB has main peaks at 1590, 1491 and 1295 cm^{-1}, corresponding to N=Q=N stretching of the quinoid rings, N-B-N stretching of the benzenoid rings and C-N-C stretching of the secondary aromatic amine, respectively [38-40]. Fig 1 (a) further shows the presence of the

characteristic peaks from PAMPSA in the PANI-PAMPSA complex (powder). It confirms successful in-situ synthesis and doping: the peaks at 1030 and 1145 cm^{-1} correspond to the symmetric S=O stretching and asymmetric SO_3^- stretching of the sulfonic acid group and the peak near 1653 cm^{-1} is the C=O stretching in PAMPSA [41-44]. The quinoid ring peak at 1590 cm^{-1} in the PANI-EB showed a noticeable shift to approximately 1564 cm^{-1} in the PANI-PAMPSA. This indicates that there was an interaction between the π-conjugated quinoid structure of PANI and sulfonic acid group of PAMPSA, associated with the degree of charge delocalisation on the polymer backbone [40].

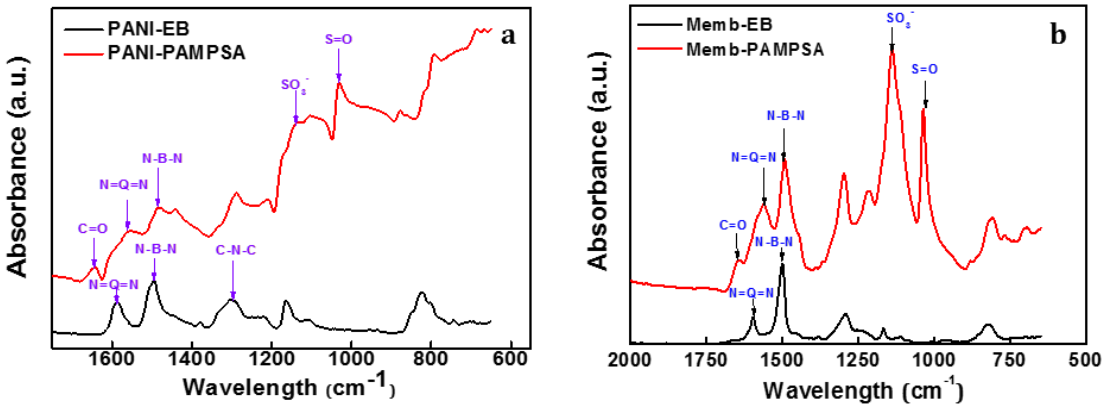

Fig. 1 (a) FTIR spectra of the PANI-PAMPSA complex (powder) and PANI-EB, (b) FTIR spectra of the PANI-PAMPSA membrane and PANI-EB membrane (Memb-PAMPSA represents PANI-PAMPSA membrane; Memb-EB represents PANI-EB membrane).

Fig 1 (b) compares the FTIR spectra of PANI-PAMPSA membrane and PANI-EB membrane. The peaks from the complex are retained. The main absorption peaks of the quinoid and benzenoid rings appeared at 1498 cm^{-1} and 1598 cm^{-1} in PANI-EB membrane, and at 1495 cm^{-1} and 1578 cm^{-1} in the PANI-PAMPSA membrane. Peaks in the PANI-PAMPSA membrane at approximately 1030 cm^{-1} and 1653 cm^{-1} correspond to the S=O stretching of the sulfonic acid group and C=O stretching, respectively. The peak at 1148 cm^{-1} was assigned to asymmetric SO_3^- stretching, which is representative of sulfonate salts. This peak was broader, probably due to

overlapping with the vibrational band of the nitrogen quinone [31]. Overall, the presence of the characteristic FTIR peaks of the PANI-PAMPSA membrane confirms interactions between the imine nitrogen of PANI and the sulfonic acid groups of PAMPSA. Moreover, EDS analysis (Fig S5 in the Supplementary material) further confirms the incorporation of PAMPSA into the PANI structure.

3.1.3 Morphology of the PANI-PAMPSA complex (powder) and PANI-PAMPSA membrane

Fig. 2 shows the FESEM images of the PANI-PAMPSA complex (powder) (Fig. 2 (a, c, e)) and PANI-EB (Fig. 2 (b, d, f)) for comparison. Fig S6 (Supplementary material) shows the FESEM images of the four different PANI-PA complexes and PANI-EB for comparison. As can be observed, each PA resulted in different morphologies. However, as stated in Section 2.3.1, only PANI-PAMPSA and PANI-EB were able to form a membrane, and thus only the formed membranes will be discussed further. PANI-EB synthesised using HCl had a granular morphology, which is typical for PANI prepared in a strongly acidic solution [45]. The PANI-PAMPSA complex (powder) however produced a fibrous network, confirming previous findings [29]. The differences in morphology are due to the dopants, with the fibrous network formed due to the strong interaction between -SO_3 of PAMPSA and the conjugated structure of PANI, as well as the possible hydrogen bonding between the –NH groups of PAMPSA and the unsaturated nitrogen atoms of PANI (–NH···N=) [42]. It was also observed that the PANI-PAMPSA complex (powder) was harder to grind and much more rigid than PANI-EB, which may indicate a stronger molecular association between PANI and PAMPSA. The different morphologies formed by the incorporation of PAMPSA should make the membranes formed different to conventional PANI membranes.

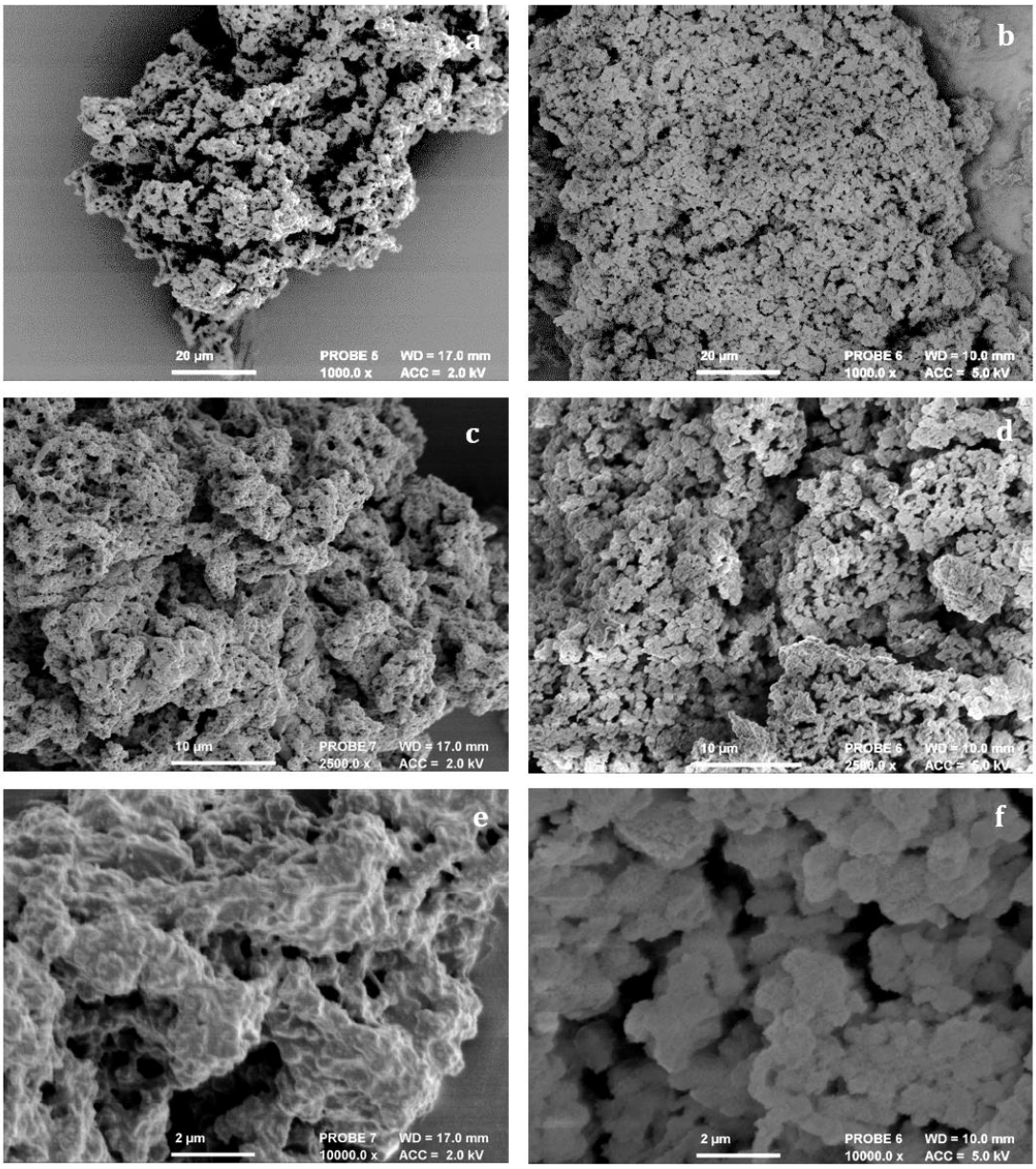

Fig. 2 FESEM images of (a, c, e) PANI-PAMPSA (left) and (b, d, f) PANI-EB (right) with scale bars of 20, 10 and 2 µm (top to bottom).

Error! Reference source not found. shows the SEM images of the PANI-PAMPSA membrane and PANI-HCl membrane. Some coiled-like PANI-PAMPSA complex (powder) can be observed on the membrane surface. The PANI-PAMPSA membrane is more porous and loose in contrast to the PANI-HCl membrane. The PANI-HCl membrane has a tighter structure showing three layers: a denser skin layer, a transition region and a relatively porous layer on the PP/PE backing layer

[46]. This suggests that the use of larger dopants produced greater intermolecular spacing between the PANI polymer chains and clusters and therefore expanded the membrane pore structures, and facilitated the formation of a loose membrane with higher porosity and larger pore size.

It can further be observed (Fig 3 (e-f)) that the growth of finger-like macrovoids was restricted in the PANI-PAMPSA membrane, which is advantageous as, finger-like macrovoids are undesirable as they weaken the mechanical strength of membranes [47, 48]. These results further confirm that incorporating PAMPSA into PANI membranes can improve their mechanical properties.

Generally, the formation of finger-like macrovoids can be hindered by increasing the polymer concentration in the polymer solution, increasing solvent evaporation time and/or choosing a solvent/non-solvent pair with low miscibility [49]. Although the same concentration of polymer was used in the NIPS method, the PANI-PAMPSA formed a more viscous casting solution than PANI-EB, which is in part due to a different dissolution in the solvent. The viscosity of the solution influence the convective flows and the demixing process and thus the formation of microstructures. A greater viscous hindrance slows down the precipitation rate, inhibiting the formation of finger-like macrovoids [49]. In addition, PANI-PAMPSA is more hydrophilic than the PANI-EB [20], and need a longer time to coagulate in the water bath to form the films. A slower coagulation rate is desirable to form membranes with “sponge-like” substructures [50].

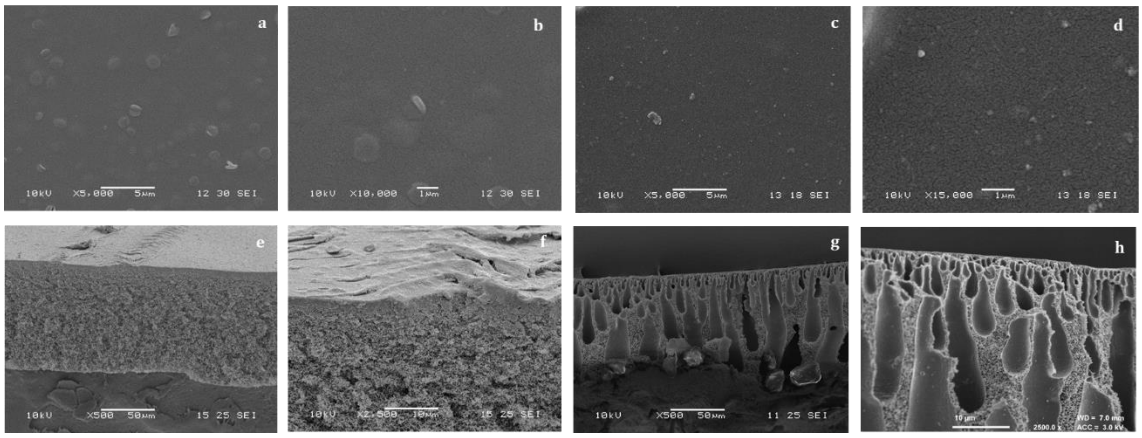

Fig. 3 SEM images of (a, b) the surface (top) and (e, f) cross-section (bottom) of PANI-PAMPSA membrane, and (c, d) the surface (top) and (g, h) cross-section (bottom) of PANI-HCl membrane.

3.1.4 Mechanical strength of PANI-PAMPSA and PANI-HCl membranes

Fig. **4** shows the Young's modulus and tensile strength of the PANI-PAMPSA membrane and the PANI-HCl membranes. PANI-PAMPSA membranes had twice Young's modulus and tensile strength as PANI-HCl membranes, indicating the mechanical strength of the membrane is improved by the PANI-PAMPSA complex. This is due to both the plasticisation effect caused by PA (due to the ionic bonds and double-stranded network between polymer acids and PANI chains [18]) and the decrease in finger-like voids in the PANI-PAMPSA membrane (**Error! Reference source not found.**).

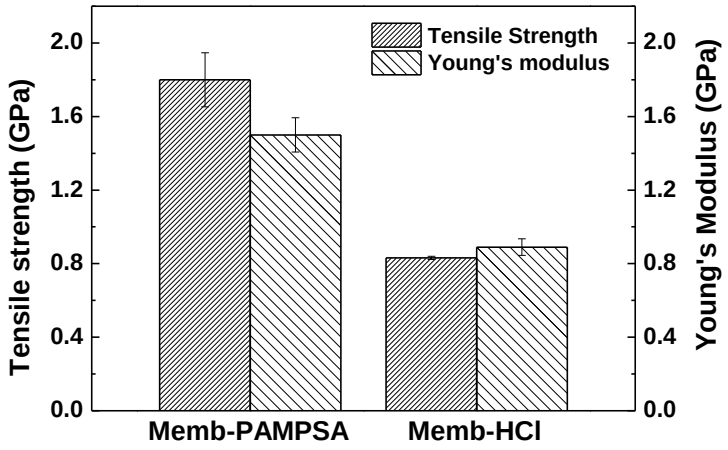

Fig. 4 Young's modulus and tensile strength of PANI-PAMPSA membrane and PANI-HCl membrane (Memb-PAMPSA represents PANI-PAMPSA membrane; Memb-HCl represents PANI-HCl membrane).

It was also observed during the experiment that the PANI-PAMPSA membrane was less brittle and easier to handle in comparison to PANI-HCl membrane. Improved durability and flexibility were also reported by previous researchers for conventionally synthesised PA membranes [18]. Above all, it can be concluded that the produced PANI-PAMPSA membrane possesses good mechanical strength: it is less brittle and more flexible than small-acid doped membranes.

3.1.5 Stability of PANI-PAMPSA and PANI-HCl membranes in filtration

To determine the extent of acid dopant leaching and test the membrane stability, the pH of the membrane permeates from different filtration stages were measured. An average of three membrane samples was recorded and standard deviation was reported. Fig. 5 shows the pH of the permeate (before filtration, after preconditioning and after filtration) of the PANI-PAMPSA membrane and PANI-HCl membrane in dead-end filtration. It can be observed that the permeate pH of the PANI-HCl membrane decreased during filtration, indicating that HCl had been leached out. However, the permeate pH of the PANI-PAMPSA membrane was stable, indicating that the fabrication method of the PANI-PAMPSA membrane overcame the acid leaching problem and was therefore more stable during filtration. This indicates that the interwoven and/or double-stranded structure aimed for in the PANI-PAMPSA complex likely binds the acid more strongly and thus there is no loss of PAMPSA during the filtration. This is in accordance with the previous studies in PANI-PA complexes [16, 25].

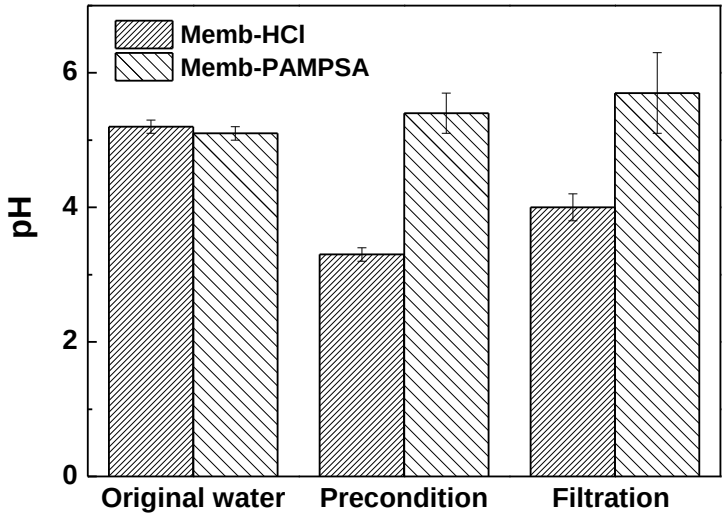

Fig. 5 pH change of PANI-PAMPSA membrane and PANI-HCl membrane in dead-end filtration (Memb-PAMPSA represents PANI-PAMPSA membrane; Memb-HCl represents PANI-HCl membrane).

3.1.6 Electrical conductivity of PANI-PAMPSA and PANI-HCl membranes

Fig. 6 shows the electrical conductivity of PANI-PAMPSA membrane and PANI-HCl membrane before and after filtration (both for water and PEG mixture as feed). The conductivity of a virgin PANI-HCl membrane was two orders of magnitude higher than the PANI-PAMPSA membrane. The PANI-HCl, however, exhibited a four orders of magnitude decrease in conductivity after water and PEG filtration. The conductivity of the PANI-PAMPSA membrane also decreased after filtration but remained in the same order of magnitude as the virgin membranes. This further confirms that the stronger interaction between PANI and PAMPSA formed during the in-situ polymerisation is able to overcome the leaching of the dopant acid.

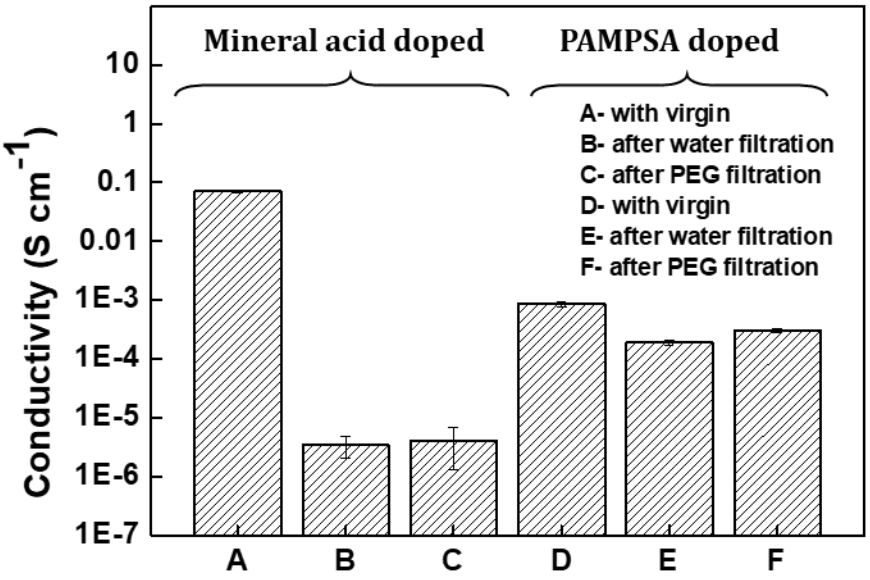

Fig. 6 Electrical conductivity of PANI-PAMPSA membrane and PANI-HCl membrane before and after dead-end filtration (A, B and C represent PANI-HCl membranes - virgin, after water filtration and after PEG filtration respectively; D, E and F represent PANI-PAMPSA membranes - virgin, after water filtration and after PEG filtration respectively).

3.1.7 Separation properties of PANI-PAMPSA and PANI-HCl membranes

Fig. 7 shows that the permeance of the PANI-PAMPSA membrane (both for water and PEG mixture as feed) was significantly higher than PANI-HCl membrane. The rejection of PEG 6000 (MW=6000 g mol^{-1}) of the PANI-PAMPSA membrane was 32% whilst for the PANI-HCl membrane, the PEG 6000 rejection was 84% under the same operating conditions (Fig S7 in the Supplementary material). This shows that the incorporation of PAMPSA formed membranes with a loose structure and high porosity. BSA (MW of 66,000 g mol^{-1}) was completely rejected by the PANI-PAMPSA membrane, indicating that the MWCO of the PANI-PAMPSA membrane was higher than 6000 g mol^{-1} but less than 66,000 g mol^{-1}.

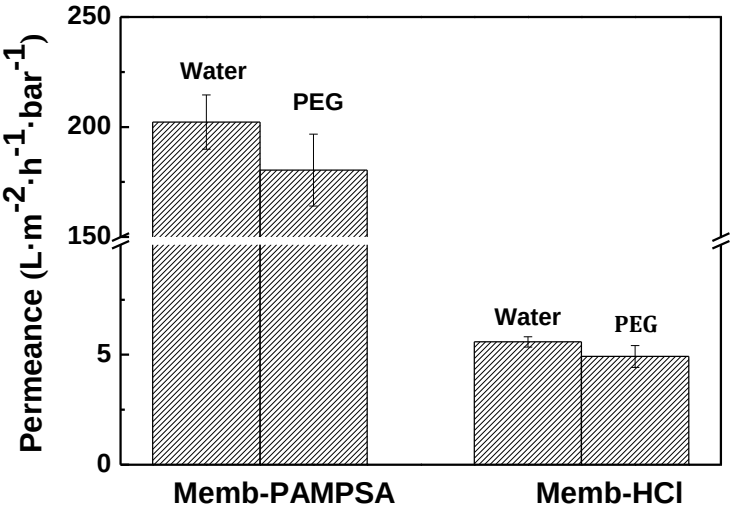

Fig. 7 Permeance of PANI-PAMPSA membrane and PANI-HCl membrane in dead-end filtration (Memb-PAMPSA represents PANI-PAMPSA membrane; Memb-HCl represents PANI-HCl membrane).

3.2 Tuneable membrane filtration and fouling removal using PANI-PAMPSA membranes

3.2.1 Tuneable transport properties

To determine if the membranes have electrically tuneable properties, PANI-PAMPSA membranes were evaluated in electrically connected cross-flow filtration using the PEG mixture [37]. Pre-conditioning of the membranes was not performed (unlike the dead-end filtrations) in order to determine if the virgin membranes showed performance change with time in cross-flow filtration. Please note that this was done for the water feed only. The permeance decreased due to the precondition of membranes at the beginning of the experiment. The external potential was applied to the membrane surface when the water flux across the membrane was stable after 2 h.

The rejection of PANI-PAMPSA membranes at different filtration times (0, 30, 60 and 120 min) under applied potentials (0 and 30 V) was compared (Fig S8 in the Supplementary material). It was found that the rejection of PEG solute mixtures

decreased in the presence of external electrical stimuli. Note that the drop in rejection with applied potential is opposite to what was observed for PANI-HCl membranes which indicates an increase in PEG rejection [14] (Fig S9 in the Supplementary material). The PANI-PAMPSA membrane structure therefore became more open/porous while PANI-HCl membrane structure tightened by the application of external voltage as previously investigated in our group [14].

The permeance and current of PANI-PAMPSA membranes with two kinds of feed (PEG mixture Fig. 8 (a) and water Fig. 8 (b)) with and without applied potential were measured to evaluate the membrane tuneability as well as the filtration stability. The permeance increased with applied voltage in both cases as shown in Fig. 8, further indicating the electrical tuneability of these membranes. The flux change of the PEG mixture was larger than that of water under the applied potential. One possible reason could be the mobility of the charge carriers (facilitation of charge transfer and electron movement along the polymer chain) in the PANI-PAMPSA membrane by PEG solution when the electrical potential was applied. PEG has been known to influence and enhance the electrical charge carrier mobility in different solutions [51] and solid polymer electrolyte films [52], so this relative increase in permeance of PEG solution compared to pure water under the applied potential can be potentially related to the presence of the PEG molecules.

The current passing through the PANI-PAMPSA membrane remained stable over the course of the experiment, in contrast to the PANI-HCl membrane where the current showed a significant decrease (Fig S10 in the Supplementary material). This is consistent with the filtration pH stability results in Section 3.1.5 and Section 3.1.6, further indicating that the PAMPSA has stabilised the membranes.

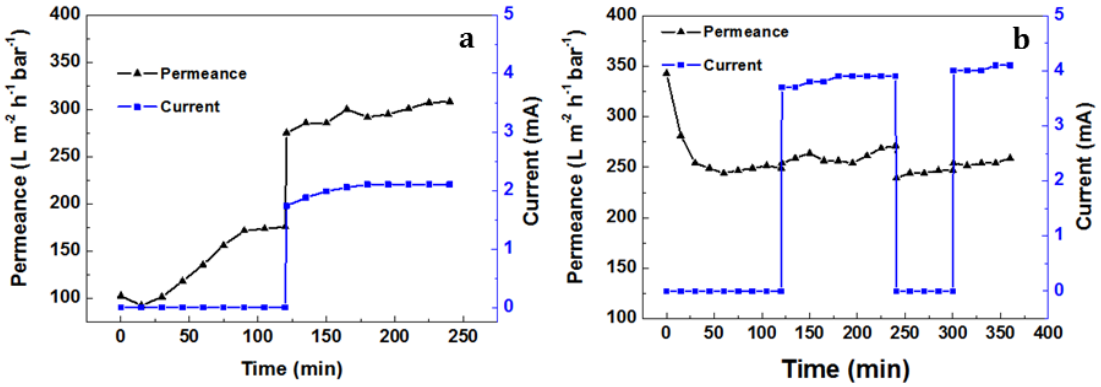

493

494 Fig. 8 Water permeance and current of PANI-PAMPSA membranes under applied potential (0 and
495 30 V): (a) PEG mixture as feed and (b) water as feed (2 bar, 25°C).

496 It is hypothesised that several properties changes in PANI-PAMPSA membrane
497 contribute to the tuneable separation under applied potential affecting the three
498 main transport mechanisms through these membranes: solution diffusion, pore
499 flow and Donnan Exclusion.

500 The applied potential is expected to facilitate the electron movement along the
501 polymer chain, generating the charge transfer between conducting domains. This
502 would affect the interaction between the solutes and membranes, influencing
503 solute transport by solution diffusion. The different charge transfer interactions
504 between PAMPSA and HCl may in part be responsible for the difference in
505 rejection behaviour with applied potential.

506 The applied potential facilitates the mobility of charged ions in the membrane,
507 which in turn changes the pore size in the membrane structure due to polymer
508 swelling. The changeable(swelled) structure influences the selectivity and
509 transportation of neutral solutes, producing membranes with tuneable separation
510 [13]. Increasingly positive membrane potentials lead to increasingly higher flux
511 values. The presence of doping acids induce charged species on PANI backbone
512 and presence of these charged species could affect the pore size of these
513 membranes and leads to changes in permeance. Compared with small-acids,

PAMPSA is a flexible polymer acid with a large benzene ring sulfonyl groups, and thus would allow for a larger void formation associated with greater pore size when it arranges its structure under electrical potential. Greater pore size provides more space for the solutes to pass through the membrane producing the decrease in rejection.

3.2.2 In-situ fouling removal under applied potential

The PANI-PAMPSA membranes can also potentially be used for fouling removal and to investigate this, BSA pre-fouled membranes were used. Fig. **9** (a) shows that after cleaning under applied potential, the water permeance improved (up to 47% of the initial flux). Fig 9 (b) further shows the steady increase of BSA concentration in the wash solution with time, which was due to the removal of the fouling under applied potential. It can be concluded that the presence of applied potential promoted the removal of BSA fouling, showing that tuneable membranes indeed have potential to be used for membrane fouling removal. The control experiment was run on BSA fouled PANI-PAMPSA membrane in the absence of applied potential and showed that the wash solution did not change (Fig S11 in the Supplementary material). This confirms that the fouling removal only occurred on the conductive membrane under applied potential.

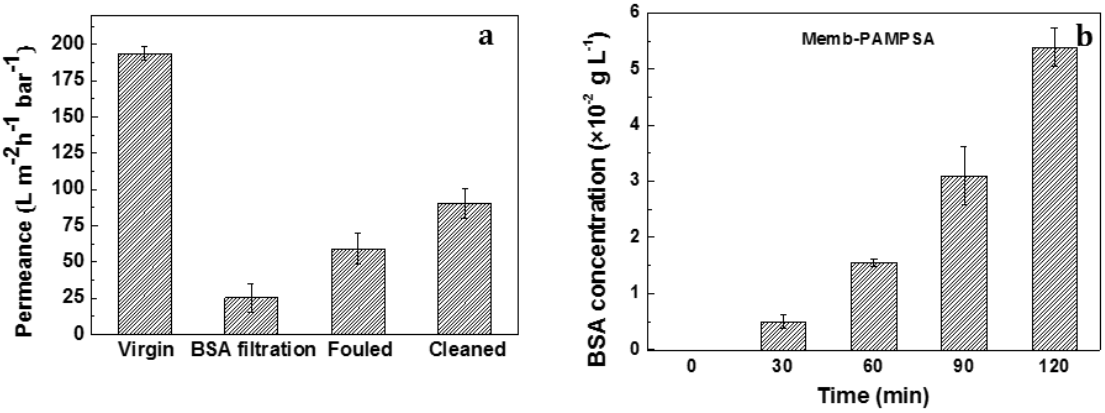

Fig. 9 (a) Permeance of PANI-PAMPSA membrane (virgin, BSA filtration, fouled and cleaned). (b) BSA concentration in the wash solution of PANI-PAMPSA membrane with time.

To further confirm the cleaning under applied potential, SEM and CLSM imaging of the virgin, fouled and cleaned membranes were done. Fig. **10** illustrates the surface difference among virgin, fouled and cleaned PANI-PAMPSA membranes, showing that the cleaning by electric potential was effective – both SEM and CLSM images illustrate that the fouling layer was reduced. FTIR analysis (Fig S12 in the Supplementary material) was also consistent with these results, suggesting that the applied potential can promote the membrane fouling removal.

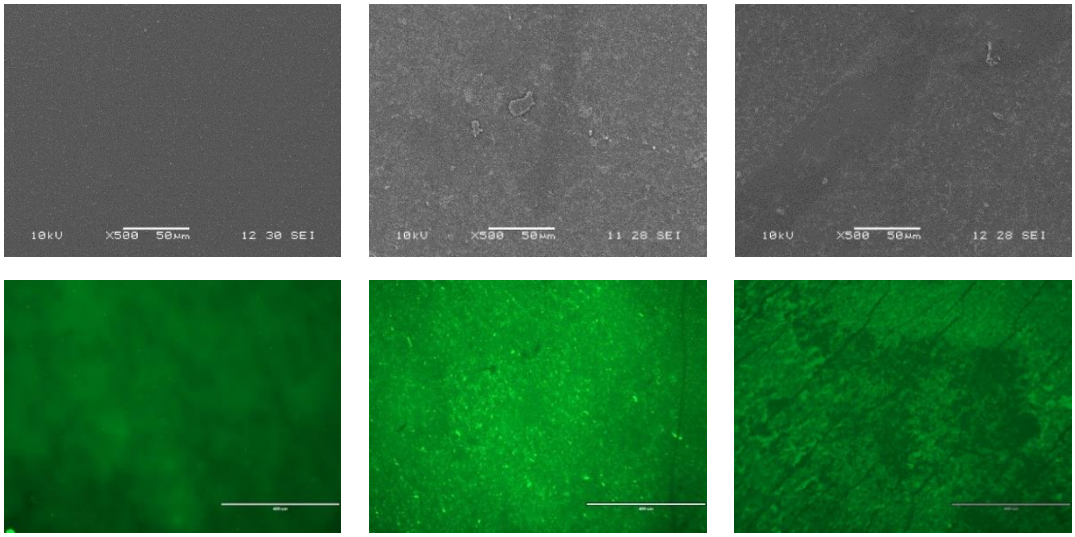

PANI-PAMPSA membrane-Virgin | PANI-PAMPSA membrane-Fouled | PANI-PAMPSA membrane-Cleaned

Fig. 10 SEM and CSLM images (top to bottom) of virgin, BSA fouled and cleaned (left to right) PANI-PAMPSA membrane with scale bar of 50 and 400 µm respectively.

Regarding the in-situ fouling removal mechanism, previous studies have shown that an externally applied electrical potential could trigger in-situ fouling removal on the electrically conductive membranes. This was attributed to two possible mechanisms [53-55].

(1) The electrically conductive membrane serves as working electrodes on applying electrical potential. The water can be electrolysed into hydrogen and

oxygen molecules upon electrical potential. The generated gas bubbles at the interface of foulants and membranes can force the deposited BSA to detach from the solid-liquid interface, and attach to the liquid-vapour interface a concept well known as froth cleaning. In this way, the protein at the liquid-vapour interface can be washed away while the protein at the solid-liquid interface stays on the membrane surface [54, 56].

(2) The applied current across the conductive membrane provides a large number of free electrons, causing direct or indirect oxidation of foulants (e.g. BSA) on the membrane surface [57]. The electrolytic oxidation can lead to the degradation or dehydration of foulants like protein, resulting in the release of deposited contaminants from membrane surface.

However, since these membranes are electrically tuneable, additional mechanisms may also help to remove the foulants. An electrically conductive PANI membrane could be dynamically responsive by applying an electrical potential across the membrane e.g., changing membrane pore size controlling pore flow transport, changing surface charge controlling Donnan exclusion, and changing membrane chemical property controlling solution diffusion. As neutral species were used in the tuneability test, so Donnan exclusion could be excluded as a reason for the electrical tuneability. The possible mechanism could be the change in pore size that resulted in a changeable permeance and rejection under applied potential. Overall this indicates that polymer acid doped PANI membranes are stable and promising candidates for in-situ removal of fouling.

4 Conclusions

A novel fabrication method to increase the acid dopant binding of poly acid (2-acrylamido-2-methyl-1-propanesulfonic acid; PAMPSA) doped into PANI

membranes has been demonstrated using in-situ synthesised polymer acid doped PANI. This is a novel way to prepare acid doped PANI membranes by allowing PAs to be primary dopants and polymerising aniline on the template of PAs. The conductivity of the obtained PANI-PAMPSA complex (powder) (1.2×10^{-1} S cm^{-1}) was three orders of magnitude higher than that formed by post synthesis PAMPSA doping (3.0×10^{-4} S cm^{-1}), indicating that this new approach was more effective in incorporating PAMPSA into the PANI structure. The in-situ synthesised PANI-PAMPSA complex produced smooth and integral membranes that addressed two of the main problems with conventional small-acid doped PANI membranes: brittleness and leaching of acid dopant. The PANI-PAMPSA membrane had a Young's modulus and tensile strength twice that of small-acid doped PANI membranes and permeate pH during filtration remained more stable compared to conventional small-acid doped PANI membranes.

The developed membranes were tested for electrical tuneability using different molecular weight PEG solution and for anti-fouling properties using BSA foulant solution. For the electrical tuneability, a higher permeance and lower rejection of PEG solution (non-ionic species) were observed under applied potential, suggesting that the membrane structure can be tuned by applying the external potential. For the anti-fouling behaviour, application of an electrical potential induces fouling removal from the membrane, with flux recovered to 47% of the initial flux and increased concentration of BSA in the wash solution.

These new PANI-PAMPSA membranes therefore provide the first step towards developing stable electrically tuneable membranes that can be robustly applied to extend the current range of membrane applications, including externally tuneable separations and in-situ removal and control of fouling.

5 Acknowledgements

The authors acknowledge the financial support of the European Research Council (ERC) Consolidator grant TUNEMEM (Project reference: 646769; funded under H2020-EU.1.1. - EXCELLENT SCIENCE).

The authors thank the University of Bath for the Overseas University Research Scholarship that funded Lili Xu's PhD. The authors thank Nicholas low for his advice on the manuscript. The authors also thank the following at the University of Bath for technical support: Daniel Lou-Hing, Fernando Acosta, Suzanne Barkley, Alexander Cuipa, Robert Brain and John Bishop.

References

[1] F. Meng, S.-R. Chae, A. Drews, M. Kraume, H.-S. Shin, F. Yang, Recent advances in membrane bioreactors (MBRs): membrane fouling and membrane material, Water research, 43 (2009) 1489-1512.

[2] A. Drews, Membrane fouling in membrane bioreactors—characterisation, contradictions, cause and cures, Journal of membrane science, 363 (2010) 1-28.

[3] R.B. Kaner, Gas, liquid and enantiomeric separations using polyaniline, Synthetic metals, 125 (2001) 65-71.

[4] Z. Liu, W. Wang, R. Xie, X.-J. Ju, L.-Y. Chu, Stimuli-responsive smart gating membranes, Chemical Society Reviews, 45 (2016) 460-474.

[5] D. Wandera, S.R. Wickramasinghe, S.M. Husson, Stimuli-responsive membranes, Journal of Membrane Science, 357 (2010) 6-35.

[6] D. Roy, J.N. Cambre, B.S. Sumerlin, Future perspectives and recent advances in stimuli-responsive materials, Progress in Polymer Science, 35 (2010) 278-301.

[7] M.A.C. Stuart, W.T. Huck, J. Genzer, M. Müller, C. Ober, M. Stamm, G.B. Sukhorukov, I. Szleifer, V.V. Tsukruk, M. Urban, Emerging applications of stimuli-responsive polymer materials, Nature materials, 9 (2010) 101-113.

[8] T. Hery, V.-B. Sundaresan, Ionic redox transistor from pore-spanning PPy(DBS) membranes, Energy & Environmental Science, 9 (2016) 2555-2562.

[9] A. Ronen, S.L. Walker, D. Jassby, Electroconductive and electroresponsive membranes for water treatment, Reviews in Chemical Engineering, 32 (2016) 533-550.

[10] G. Jeon, S.Y. Yang, J. Byun, J.K. Kim, Electrically Actuatable Smart Nanoporous Membrane for Pulsatile Drug Release, Nano Letters, 11 (2011) 1284-1288.

[11] M. Sairam, S.K. Nataraj, T.M. Aminabhavi, S. Roy, C.D. Madhusoodana, Polyaniline Membranes for Separation and Purification of Gases, Liquids, and Electrolyte Solutions, Separation & Purification Reviews, 35 (2006) 249-283.

[12] J. Pellegrino, The Use of Conducting Polymers in Membrane ‐ Based Separations, Annals of the New York Academy of Sciences, 984 (2003) 289-305.

[13] R. Rohani, Linking the Microstructural and Separation Properties of Electrically Tuneable Polyaniline Pressure Filtration Membranes, in, University of Auckland, 2013.

[14] L. Xu, S. Shahid, A.K. Holda, E.A.C. Emanuelsson, D.A. Patterson, Stimuli responsive conductive polyaniline membrane: In-filtration electrical tuneability of flux and MWCO, Journal of Membrane Science, 552 (2018) 153-166.

[15] J. Tarver, J.E. Yoo, T.J. Dennes, J. Schwartz, Y.-L. Loo, Polymer acid doped polyaniline is electrochemically stable beyond pH 9, Chemistry of Materials, 21 (2008) 280-286.

[16] H. Hu, J.M. Saniger, J.G. Bañuelos, Thin films of polyaniline–polyacrylic acid composite by chemical bath deposition, Thin Solid Films, 347 (1999) 241-247.

[17] S.-A. Chen, H.-T. Lee, Structure and properties of poly (acrylic acid)-doped polyaniline, Macromolecules, 28 (1995) 2858-2866.

[18] B.D. Malhotra, S. Ghosh, R. Chandra, Polyaniline/Polymeric acid composite, a novel conducting rubber, Journal of Applied Polymer Science, 40 (1990) 1049-1052.

[19] A.A. Nekrasov, O.L. Gribkova, V.F. Ivanov, A.V. Vannikov, Electroactive films of interpolymer complexes of polyaniline with polyamidosulfonic acids: advantageous features in some possible applications, Journal of Solid State Electrochemistry, 14 (2010) 1975-1984.

[20] J.E. Yoo, J.L. Cross, T.L. Bucholz, K.S. Lee, M.P. Espe, Y.-L. Loo, Improving the electrical conductivity of polymer acid-doped polyaniline by controlling the template molecular weight, Journal of Materials Chemistry, 17 (2007) 1268-1275.

[21] I.J. Ball, S.-C. Huang, R.A. Wolf, J.Y. Shimano, R.B. Kaner, Pervaporation studies with polyaniline membranes and blends, Journal of Membrane Science, 174 (2000) 161-176.

[22] H. Hu, J.L. Cadenas, J.M. Saniger, P. Nair, Electrically conducting polyaniline–poly (acrylic acid) blends, Polymer International, 45 (1998) 262-270.

[23] L. Zhang, H. Peng, J. Sui, P.A. Kilmartin, J. Travas-Sejdic, Polyaniline nanotubes doped with polymeric acids, Current Applied Physics, 8 (2008) 312-315.

[24] Y. Kang, M.-H. Lee, S.B. Rhee, Electrochemical properties of polyaniline doped with poly (styrenesulfonic acid), Synthetic metals, 52 (1992) 319-328.

[25] L. Sun, H. Liu, R. Clark, S.C. Yang, Double-strand polyaniline, Synthetic metals, 84 (1997) 67-68.

[26] M.F. Rubner, S.K. Tripathy, J. Georger Jr, P. Cholewa, Structure-property relationships of polyacetylene/polybutadiene blends, Macromolecules, 16 (1983) 870-875.

[27] J. Hwang, S. Yang, Morphological modification of polyaniline using polyelectrolyte template molecules, Synthetic Metals, 29 (1989) 271-276.

[28] R. Nagarajan, S. Tripathy, J. Kumar, F.F. Bruno, L. Samuelson, An enzymatically synthesized conducting molecular complex of polyaniline and poly (vinylphosphonic acid), Macromolecules, 33 (2000) 9542-9547.

[29] A. Nekrasov, O. Gribkova, T. Eremina, A. Isakova, V. Ivanov, V. Tverskoj, A. Vannikov, Electrochemical synthesis of polyaniline in the presence of poly (amidosulfonic acid) s with different rigidity of polymer backbone and characterization of the films obtained, Electrochimica Acta, 53 (2008) 3789-3797.

[30] N.V. Blinova, J. Stejskal, M. Trchová, G. Ciric-Marjanovic, I. Sapurina, Polymerization of aniline on polyaniline membranes, The Journal of Physical Chemistry B, 111 (2007) 2440-2448.

[31] S. Jeong Kim, N. Rae Lee, B.J. Yi, S.I. Kim, Synthesis and characterization of polymeric acid‐doped polyaniline interpenetrating polymer networks, Journal of Macromolecular Science Part A: Pure and Applied Chemistry, 43 (2006) 497-505.

[32] M. Sairam, X. Loh, Y. Bhole, I. Sereewatthanawut, K. Li, A. Bismarck, J. Steinke, A. Livingston, Spiral-wound polyaniline membrane modules for organic solvent nanofiltration (OSN), Journal of Membrane Science, 349 (2010) 123-129.

[33] X. Loh, M. Sairam, A. Bismarck, J. Steinke, A. Livingston, K. Li, Crosslinked integrally skinned asymmetric polyaniline membranes for use in organic solvents, Journal of Membrane Science, 326 (2009) 635-642.

[34] X.X. Loh, M. Sairam, J.H. Steinke, A.G. Livingston, A. Bismarck, K. Li, Polyaniline hollow fibres for organic solvent nanofiltration, Chemical communications, (2008) 6324-6326.

[35] A. Ohtani, M. Abe, M. Ezoe, T. Doi, T. Miyata, A. Miyake, Synthesis and properties of high-molecular-weight soluble polyaniline and its application to the 4MB-capacity barium ferrite floppy disk's antistatic coating, Synthetic Metals, 57 (1993) 3696-3701.

[36] Y. Moo Lee, S. Yong Nam, S. Yong Ha, Pervaporation of water/isopropanol mixtures through polyaniline membranes doped with poly (acrylic acid), Journal of membrane science, 159 (1999) 41-46.

[37] L. Xu, S. Shahid, J. Shen, E. Emanuelsson, D.A. Patterson, A wide range and high resolution one-filtration molecular weight cut-off method for aqueous based nanofiltration and ultrafiltration membranes, Journal of Membrane Science, 525 (2017) 304–311.

[38] C. Yan, L. Zou, R. Short, Polyaniline-modified activated carbon electrodes for capacitive deionisation, Desalination, 333 (2014) 101-106.

[39] X.M. Feng, R.M. Li, Y.W. Ma, R.F. Chen, N.E. Shi, Q.L. Fan, W. Huang, One‐Step Electrochemical Synthesis of Graphene/Polyaniline Composite Film and Its Applications, Advanced Functional Materials, 21 (2011) 2989-2996.

[40] K.R. Reddy, B.C. Sin, K.S. Ryu, J. Noh, Y. Lee, < i> In situ</i> self-organization of carbon black–polyaniline composites from nanospheres to nanorods: Synthesis,

morphology, structure and electrical conductivity, Synthetic Metals, 159 (2009) 1934-1939.

[41] J. Jang, J. Ha, J. Cho, Fabrication of Water‐Dispersible Polyaniline‐Poly (4‐styrenesulfonate) Nanoparticles For Inkjet‐Printed Chemical‐Sensor Applications, Advanced materials, 19 (2007) 1772-1775.

[42] L. Hechavarría, H. Hu, M.E. Rincón, Polyaniline–poly (2-acrylamido-2-methyl-1-propanosulfonic acid) composite thin films: structure and properties, Thin Solid Films, 441 (2003) 56-62.

[43] O. Misoon, K. Seok, Effect of dodecyl benzene sulfonic acid on the preparation of polyaniline/activated carbon composites by in situ emulsion polymerization, Electrochimica Acta, 59 (2012) 196-201.

[44] J.-W. Jeon, J. O'Neal, L. Shao, J.L. Lutkenhaus, Charge storage in polymer acid-doped polyaniline-based layer-by-layer electrodes, ACS applied materials & interfaces, 5 (2013) 10127-10136.

[45] J. Stejskal, I. Sapurina, M. Trchová, E.N. Konyushenko, Oxidation of aniline: polyaniline granules, nanotubes, and oligoaniline microspheres, Macromolecules, 41 (2008) 3530-3536.

[46] D.A. Patterson, A. Havill, S. Costello, Y.H. See-Toh, A.G. Livingston, A. Turner, Membrane characterisation by SEM, TEM and ESEM: The implications of dry and wetted microstructure on mass transfer through integrally skinned polyimide nanofiltration membranes, Separation and Purification Technology, 66 (2009) 90-97.

[47] P. Sukitpaneenit, T.-S. Chung, Molecular elucidation of morphology and mechanical properties of PVDF hollow fiber membranes from aspects of phase inversion, crystallization and rheology, Journal of Membrane Science, 340 (2009) 192-205.

[48] D. Wang, K. Li, W.K. Teo, Porous PVDF asymmetric hollow fiber membranes prepared with the use of small molecular additives, Journal of Membrane Science, 178 (2000) 13-23.

[49] G.R. Guillen, G.Z. Ramon, H. PirouzKavehpour, R.B. Kaner, E. Hoek, Direct microscopic observation of membrane formation by nonsolvent induced phase separation, Journal of Membrane Science, (2013).

[50] G.R. Guillen, Y. Pan, M. Li, E.M. Hoek, Preparation and characterization of membranes formed by nonsolvent induced phase separation: a review, Industrial & Engineering Chemistry Research, 50 (2011) 3798-3817.

[51] B.M. Abu-Zied, M.A. Hussein, A.M. Asiri, Characterization, in situ electrical conductivity and thermal behavior of immobilized PEG on MCM-41, International Journal of Electrochemical Science, 10 (2015) 4873-4887.

[52] Y. Li, J. Wang, J. Tang, Y. Liu, Y. He, Conductive performances of solid polymer electrolyte films based on PVB/LiClO4 plasticized by PEG200, PEG400 and PEG600, Journal of Power Sources, 187 (2009) 305-311.

[53] H. Saveyn, P. Van der Meeren, R. Hofmann, W. Stahl, Modelling two-sided electrofiltration of quartz suspensions: importance of electrochemical reactions, Chemical engineering science, 60 (2005) 6768-6779.

[54] Z. Wu, H. Chen, Y. Dong, H. Mao, J. Sun, S. Chen, V.S.J. Craig, J. Hu, Cleaning using nanobubbles: Defouling by electrochemical generation of bubbles, Journal of Colloid and Interface Science, 328 (2008) 10-14.

[55] F. Ahmed, B.S. Lalia, V. Kochkodan, N. Hilal, R. Hashaikeh, Electrically conductive polymeric membranes for fouling prevention and detection: A review, Desalination, 391 (2016) 1-15.

[56] A. Agarwal, W.J. Ng, Y. Liu, Principle and applications of microbubble and nanobubble technology for water treatment, Chemosphere, 84 (2011) 1175-1180.

[57] C.D. Vecitis, M.H. Schnoor, M.S. Rahaman, J.D. Schiffman, M. Elimelech, Electrochemical multiwalled carbon nanotube filter for viral and bacterial removal and inactivation, Environmental science & technology, 45 (2011) 3672-3679.

List of Figures

List of Table